JAVIER VICENTE FERRAGUD ADAM; Piquero-Cilla, J.; Domenech Carbo, MT.; Guerola Blay, V.; Company Climent, J.; ANTONIO DOMÉNECH CARBÓ (2016). Electrochemical analysis of gildings in Valencia altarpieces: a cross-age study since fifteenth until twentieth century, Journal of Solid State Electrochemistry. Journal of Solid State Electrochemistry. 21(5):1477-1487. doi:10.1007/s10008-017-3512-8

Journal of Solid State Electrochemistry

Electrochemical analysis of gildings in Valencia Altarpieces: a cross-age study since 15th until 20th century

--Manuscript Draft--

Manuscript Number:	
Full Title:	Electrochemical analysis of gildings in Valencia Altarpieces: a cross-age study since 15th until 20th century
Article Type:	Original Paper
Corresponding Author:	Antonio Domenech-Carbo University of Valencia Burjassot, Valencia SPAIN
Corresponding Author Secondary Information:	
Corresponding Author's Institution:	University of Valencia
Corresponding Author's Secondary Institution:	
First Author:	Antonio Domenech-Carbo
First Author Secondary Information:	
Order of Authors:	Antonio Domenech-Carbo
	Xavier Ferragud, PhD
	Joan Piquero-Cilla, Graduate Chemistry
	María Teresa Doménech-Carbó, PhD
	Vicent Guerola-Blay, PhD
	Ximo Company, PhD
Order of Authors Secondary Information:	
Funding Information:	
Abstract:	The application of the voltammetry of microparticles methodology to the study of gildings in paintings and architectural ornaments is described. Nanosamples from pieces from different churches of the Comunitat Valenciana (Spain) covering since the 15th century until nowadays were studied upon attachment to graphite electrodes in contact with aqueous HCl and H2SO4 electrolytes. Electrochemical measurements, combined with field emission scanning electron microscopy-X-ray microanalysis (FESEM-EDX) and atomic force microscopy (AFM) data, denoted that a common manufacturing technique was used with minimal variations along time. The relationship between specific voltammetric features associated to bulk gold and active surface sites, however, changed monotonically with time, thus suggesting the possibility of age monitoring.
Suggested Reviewers:	Frank Marken, PhD Professor, University of Bath f.marken@bath.ac.uk Expertise in solid-state electrochemistry
	Philippe Dillmann, PhD Professor, Laboratoire Archéomatériaux et Prévision de l'Altération, CNRS philippe.dillmann@cea.fr Expertise in archaeological metal
	Luc Robbiola, PhD Professor, University of Toulouse robbiola@univ-tlse2.fr Expertise in archaeological metal

Electrochemical analysis of gildings in Valencia Altarpieces: a cross-age study since 15th until 20th century

Xavier Ferragud[a,b], Joan Piquero-Cilla[a], María Teresa Doménech-Carbó[b], Vicent Guerola Blay[b], Ximo Company[c], Antonio Doménech-Carbó*[a]

[a] Departament de Química Analítica. Universitat de València. Dr. Moliner, 50, 46100 Burjassot (València) Spain.

[b] Institut de Restauració del Patrimoni. Universitat Politècnica de València. Camino de Vera 14, 46022, Valencia, Spain.

[c] Departament de Història de l'Art, Universitat de Lleida

* Corresponding author, e-mail: antonio.domenech@uv.es.

Abstract

The application of the voltammetry of microparticles methodology to the study of gildings in paintings and architectural ornaments is described. Nanosamples from pieces from different churches of the *Comunitat Valenciana* (Spain) covering since the 15th century until nowadays were studied upon attachment to graphite electrodes in contact with aqueous HCl and H_2SO_4 electrolytes. Electrochemical measurements, combined with field emission scanning electron microscopy-X-ray microanalysis (FESEM-EDX) and atomic force microscopy (AFM) data, denoted that a common manufacturing technique was used with minimal variations along time. The relationship between specific voltammetric features associated to bulk gold and active surface sites, however, changed monotonically with time, thus suggesting the possibility of age monitoring.

Keywords: Gilding; Voltammetry of microparticles; FESEM-EDX; AFM; Aging.

Introduction

Gold has been used since the antiquity for jewelry, cult figures, etc. playing an important role because of its economical and symbolic values [1,2]. The use of thin laminas of gold for decorating parts of altarpieces and polychromed sculptures [3], furniture and painting frames [4] and architectural ornaments (ceilings, columns, pilasters, cornices, etc) [5-7] in churches, palaces and mansions was an extended practice since the Middle Age, involving specific techniques for the preparation of the gold leaf [8-11]. In the *Valencian Community* (Spain), this artistic technique was extensively used between the 15th and 19th centuries and the gold beating process was regulated since the 17th century, differentiating the jobs of painter and *daurador* (gilding craftsman) [12,13]. As an example, in 1616 there was a minimum of 15 authorized gilding workshops, only in the city of Valencia, [14].

Because of the extensive use of gilding in painting, sculpture, architecture and decorative arts, the knowledge of the materials and artistic techniques used for preparing gildings in the past is an essential analytical target for conservation and restoration purposes. Apart from the general problems of the analysis of archaeological objects and works of art [15], the analysis of gilded surfaces involves two particular difficulties: their constitution as a fine lamina deposited on several preparatory layers [16-18] and the chemical inertness of gold. Accordingly, few studies have been devoted to detect false gildings [19], whereas differentiation between sources of archaeological gold requires the determinations of accompanying elements at the level of traces [20].

In this context, the voltammetry of microparticles methodology (VMP), a solid-sate electrochemical technique developed by Scholz et al. [21,22] can be used as a complementary analytical tool due to its high sensitivity and requirement of amount of sample at the micro-nanogram level. This technique, which can be applied to a variety of solid materials [23-24], has been previously proposed for characterizing, tracing and dating archaeological lead [25,26], copper/bronze [27-29], and silver [30-33] objects based on the analysis of specific voltammetric features associated to the corrosion layers of the pieces attached to graphite electrodes immersed into aqueous electrolytes.

Here, we report an application of VMP for studying gilding decoration. For this purpose, a set of samples was taken from gilded surfaces of a series of altarpieces from the *Comunitat Valenciana* (Spain). The pieces studied cover a time interval ranging between the beginning of the 15th century and the modern times in order to characterize materials, determine possible differences in the manufacturing technique and provide aging data. Figure 1 shows an image of the Altarpiece of Saint Joseph located in *L'Assumpció* church of Torrent (Valencia, Spain) performed by Andreu Robres (1728), illustrating the extensive use of the gilding technique which was typical in this kind of panel pieces. Gold leaf samples from altarpieces and decorative architectural ornaments in churches accomplish two interesting characteristics: i) all samples were taken from altarpieces of well-documented date of finishing; ii) the set of altarpieces studied are located in a relatively restricted geographic area so that the conditions of aging can be considered essentially identical. The characteristics and dating of the studied samples of gilded altarpieces are summarized in Table 1 [34].

The proposed methodology is based on the record of voltammetric features associated to the electrochemical oxidation of metallic gold in contact with aqueous HCl and H_2SO_4 electrolytes. In spite of its recognized chemical stability, gold possesses a rich oxidative electrochemistry resulting in the formation of gold oxide coatings and, in the presence of complexing agents, oxidative dissolution processes [35-44]. Consistently with the observed sensitivity of the voltammetric response, including electrocatalytic effects [42-44], to the presence of surface active sites [37-41] and exposed crystal planes [42,43], it is hypothesized here that the voltammetric response of gilded surfaces should be sensitive to changes in the chemical and textural properties of the metal surface thus being able to reveal light changes in the composition of the base metal, preparation technique and aging. In order to test that hypothesis, voltammetric data were combined here with atomic force microscopy (AFM) examination of gold surfaces. Samples from gilded panels were also examined by means of field emission scanning electron microscopy with energy dispersive X-ray analysis (FESEM/EDX).

Experimental

A couple of samples were excised with the help of a microscalpel from each altarpiece studied. The samples consisted of fragments including the entire campaign of gilding (ca. 1 mg). A gilding campaign consists of an inner thick white gesso layer followed by a colored preparatory layer of bole and finally the gold leaf (Figure 2). Electrochemical experiments were performed in sample-modified graphite electrodes at 298 K in a three-electrode cell under argon atmosphere using a CH I660C device. An AgCl (3 M NaCl)/Ag reference electrode and a platinum-wire auxiliary electrode completed the conventional three-electrode arrangement. Aqueous HCl and H_2SO_4 (Panreac reagents) solutions were used as supporting electrolytes. In order to test possible effects associated to the oxygen reduction reaction (ORR), no deaeration was carried out. Cyclic and square wave voltammetries (CV and SWV, respectively) were used as detection modes. For electrode modification, graphite electrodes (Alpino HB, diameter 3 mm) were pressed, using the 'one touch' protocol [45,46] on the gold leaf in the surface of the first sample excised of each altarpiece previously immobilized on a paste bed. The modified electrode was dipped into the electrochemical cell so that only the lower end of the electrode was in contact with the electrolyte solution. This procedure provides an almost constant electrode area and reproducible background currents. Complementary experiments were performed on commercial gold leaf (Masserini, Milan, Italy) and gold electrodes (BAS MF2014, geometrical area 0.018 cm^2) before and after treating with different conditioning treatments. In order to mimic traditional techniques used in the fabrication of gilded panels, burnishing treatment until obtaining a mirror-like finishing of the gilded surface was also performed with an agate burnisher.

AFM-monitored electrochemical experiments were performed with a multimode AFM (Digital Instruments VEECO Methodology Group, USA) with a NanoScope IIIa controller and equipped with a J-type scanner (max. scan size of 150×150×6 μm). The topography of the samples was studied in tapping mode. An OTESPA-R3 probe (300kHz and 26 N/m) has been used with a V-shaped cantilever configuration.

For FESEM-EDX analysis, the second sample excised of each alterpiece was prepared as a cross-sections by embedding in polyester resin and polishing with SiC abrasive disks. Cross-sections were examined under a Zeiss model ULTRA 55 field emission scanning electron microscope, which operated with an Oxford-X Max X-ray microanalysis system. Image acquisition was done at the 3 kV accelerating voltage. The chemical

composition of pigments was obtained at the 20 kV accelerating voltage and 6-7 mm was the working distance for the X-ray detector. Samples were carbon-coated to eliminate charging effects. A semiquantitative microanalysis was carried out by the ZAF method to correct interelemental effects. The counting time was 100 s for major and minor elements alike. Element percentages were generated by the ZAF method on the Oxford-Link-Inca EDX software, which was performed to exclude C to avoid erroneous quantification because the signal detected for this element mainly came from the C coating applied to samples to suppress charge effects.

A stereoscopic light microscope Leica GZ6 (X10-X50) was used for obtaining digital images of the samples prepared as cross sections. Leica Digital FireWire Camera (DFC) with Leica Application Suite (LAS) sotftware has been used for acquiring and processing the digital images.

3. Results and discussion

3.1. Microscopy examination of samples

As previously mentioned a series of samples, which were excised of the complete set of altarpieces studied, were prepared as cross sections and examined, successively, with both optical and field emission scanning electron microscopes consisted of fragments (ca. 1 mg). The cross section prepared included the entire distribution of strata corresponding to the gilding campaign as can be seen in Figure 2-a in which is shown the cross section obtained from the sample **S9** corresponding to *El Calvari* Altarpiece in the Luis Vives Institute of Valencia dated back to 1675: the thin leaf of gold, which was burnished by the help of an agate burnisher following the traditional technique (layer 1), underneath it can be seen the foundation layer for burnished water gilding, which includes clay and animal glue (layer 2). The water gilding technique includes an internal ground of gesso: an outer thiner white gesso layer (layer 3) followed by an inner and thicker layer of gross gesso (layer 4). Figure 2-b shows the secondary electron image obtained with FESEM. In this microphotograph can be observed in detail the thickness of the gold leaf (layer 1), the layer of clayey bole (layer 2) and the outer ground layer prepared with thiner gesso grains (layer 3). Amorphous dark aggregates visible in the centre of the image in the latter are associated to the animal glue used as binding medium. The energy X-ray spectrum shown in Fig 2-c was obtained by means of an spot analysis in the gold leaf. Apart from the intense emission lines from Au, weak emission line of Ag is also present in the spectrum

that put in evidence the use of a Au-Ag alloy in this gilding. Some elements such as Fe and Ca also present in the spectrum are associated to the clayey materials from the bole layer underneath the gold leaf.

Elemental composition obtained (see Table S2 included as supplementary material) with FESEM-EDX in the bole layer of the set of gilding samples studied suggested that the studied gilding can be divided into two groups according to the type of earth pigment used as bole. As can be seen in Figure 3, for one half of samples the values of the percentages of MgO and Al_2O_3 appeared as mutually related (denoted by empty squares), the corresponding data points falling in a common curve in the diagram in percentages of Al_2O_3 below 25 wt%. The remaining samples, however, displayed alumina percentages above 25 wt% and low MgO contents with no apparent correlation between them (grey squares in Figure 3). Location of the pieces in the Valencian Community (see inset in Figure 3) indicated that the first group of samples was placed in the center (Valencia city and Torrent) and north of the region (Sogorb) with the unique exception of sample **S13** (Oliva), while the second group was placed in the south of the region (Algemesí, Alzira, Banyeres, Pego). This separation can be attributed to the use of (at least) two different clay sources for preparing the bole and suggested that the different local workshops used accessible raw materials.

In contrast, the elemental composition of the gold leaf, as determined from FESEM-EDX data, does not suggest any grouping of the samples nor correlation with the bole composition (see Figure 5). Au percentages ranged between 95.6 and 98.1 wt%, only accompanied by Ag in samples between the 15^{th} and 19^{th} centuries. Uniquely sample **S5** and the samples from the 20^{th} century presented copper in percentages between 1.1 and 4.5 % and silver in percentages between 2.2 and 5.8 wt%. Pertinent data are provided as Supplementary information (Table S1). Such data reveal that high-purity gold was used and, in principle, do not allowed for extracting conclusive grouping.

AFM examination of gold leaf (Figure 4a) revealed a smooth surface with minor roughness at the micrometer scale. Samples, in general, exhibited a similar rougher surface which was characterized by a more definite rounded features at nanoscale (Figure 4b).

3.2. General voltammetric pattern

The voltammetry of pristine polycrystalline gold electrode is illustrated in Figures 5a,b in contact with air-saturated a) 0.10 M H_2SO_4 and b) 0.10 M HCl aqueous solutions. In the initial positive-going potential scan, an anodic peak at ca. +1.2 V vs. Ag/AgCl (A_1) appeared preceding the rising current for the oxygen evolution reaction (A_{OER}). In the subsequent negative-going potential scan, a sharp cathodic peak at ca. +0.6 V (C_1) appeared. When the potential scan was prolonged to more cathodic potentials, a cathodic wave at ca. –0.2 V was recorded preceding an intense reduction current at potentials more negative than –0.5 V. The first process (C_{ORR}) is attributable to the reduction of dissolved oxygen (oxygen reduction reaction, ORR) while the second (C_{HER}) corresponded to the hydrogen evolution reaction (HER). After polishing with an agate burnisher (Figure 5c), the voltammetric response changed slightly but significantly, with lowering and broadening of the signal A_1, the enhancement of the C_{ORR} wave relative to the above, and the appearance of an ill-defined couple C_2/A_2 at potentials ca. +0.3 V. These features can be considered as illustrative of the influence of the surface treatment on the electrochemical activity of gold surfaces [42-44].

The voltammetric response of the gold leaf samples attached to graphite electrode by means of the 'one-touch' sampling [45,46] was in principle similar, processes A_1 and C_1 being also recorded accompanying A_{OER}, C_{ORR} and C_{HER} signatures. The more significant difference in the voltammetry of polycrystalline gold between HCl and H_2SO_4 electrolytes under our experimental conditions was the wave broadening observed in HCl electrolytes.

These features can be rationalized on considering the complex electrochemistry of gold in acidic aqueous solution [35-44]. In absence of complexing agents, the process A_1 can be described as the oxidation of metallic gold to form different types of oxide deposits, monolayer, and hydrous. The standard electrode potential for the process:

$$Au + 3H_2O \rightarrow Au_2O_3 + 6H^+_{aq} + 6e^- \quad (1)$$

is of 1.51 V vs. SHE for the anhydrous oxide (or α-oxide) and +1.46 V for the hydrated oxide (or β-oxide) [38,39]. It is believed that the early stage of the electrochemical oxidation of polycrystalline gold consists of the formation of some type of metal-hydroxy compound, *eg.* $Au^{\delta+}$... $OH^{\delta-}$ from which forms an adherent monolayer of compact material. The β-oxide, having low density and porous nature would growth subsequently. The process C_1, often resolved in two consecutive peaks, corresponds to the reduction of the generated oxide forms to gold metal. This process occurs at potentials remarkably different from those of process A_1, a situation often termed as hysteresis, which can be interpreted assuming that the reduction of oxide forms yields displaced surface atoms (Au*), which are in a state of still higher activity than regular surface atoms as a result of their generation in a state of unusually low lattice coordination number. Following Burke et al. [35,38,39], the electrochemical runs involve a place-exchange process where the surface metal atoms switch positions with adsorbed oxygen species leading to a considerable reduction of the electrostatic repulsion energy and resulting in the lowering of the reduction potential. In this context, the signals A_2/C_2 can be attributed to active surface sites which are electrochemically generated at cathodic potentials [38,39,42,43]. In HCl, the oxidation of gold involves to some extent the dissolution via formation of Au-chloride complexes ($AuCl_4^-$ mainly) and peculiar activation/catalytic effects have been reported [42,47,48].

3.3. Voltammetry of gilded panels

Figure 6 compares the CVs after semi-derivative deconvolution of an unmodified graphite electrode (a) with those for electrodes modified with gold leaf (b) and sample **S6** (c) in contact with 0.10 M HCl. The bare graphite does not showed any of the gold-localized signals previously described whereas the gold leaf showed the aforementioned peaks A_1 and C_1 attributed to 'bulk' gold. In contrast, the initial anodic scan voltammogram of the panel sample provided relatively intense an additional peak A_2 at ca. +0.45 V preceding the signal A_1 at ca. +1.1 V while in the subsequent cathodic scan, the peak C_1 was accompanied by a second cathodic signal C_2. Two remarkable features can be underlined: i) The signal A_2 appeared in panel samples even if the potential is initiated at 0.0 V (i..e., at potentials where no electrochemical activation of gold occurs at polycrystalline electrodes, *vide infra*), and ii) the signal A_2 was enhanced in the

second and successive scans in CVs (Figure 6c) when the potential is switched at values more negative than –0.2 V.

As previously indicated, these features can be interpreted, following Burke and O'Mullane [38], on assuming that the anodic response of polycrystalline gold corresponds to the oxidation of very active gold atoms at the surface of the gold leaf, a process which can be described as a combination of oxidation, hydration and hydrolysis [35]:

$$\mathrm{Au}^{*} \xrightarrow{-3e^{-}} \mathrm{Au}^{3+} \xrightarrow{+(n+3)\mathrm{H_2O}} \mathrm{Au}^{3+}\cdot(n+3)\mathrm{H_2O} \xrightarrow{-3\mathrm{H}^{+}} \mathrm{Au(OH)_3}\cdot n\mathrm{H_2O} \qquad (2)$$

At polycrystalline gold electrodes, the A_2/C_2 couple appears only after cathodic polarization at potentials below 0.0 V [38,39,42,43], being attributed to the oxidation/reduction of active Au sites. This feature was also observed in the voltammograms of gilded panels, polycrystalline gold and gold leaf; however, only in the gilded panel samples the A_2/C_2 couple appears without previous cathodic polarization. This feature can be associated to the presence of active Au sites as a result of the interaction of the surface of the gold leaf with the environment and eventually the presence of impurities, adsorbates, etc. Tentatively, the increased presence of active Au* sites in aged samples, can be considered as supported by AFM images in Figure 4. Although the overall roughness of the surface of the gold leaf at macroscopic scale would be similar, the surface of the aged gold foils present a more sharp boundary between the protruding features, which can be associated to such active sites.

3.4. Electrochemical age markers

Figure 7 depicts SWVs of polycrystalline gold electrode abrasively conditioned and graphite electrodes modified with gold leaf samples, also abrasively conditioned using an agate burnisher (mimicking the burnishing procedure used in traditional techniques for conditioning gilded panels), sample **S10**, dated back in 1723, and sample **S1**, dated in 1405, in contact with air-saturated 1.0 M H_2SO_4. In the positive-going potential scan, both the bold electrode and the gold leaf displayed an intense peak A_1 preceded by several overlapping signals between +0.2 and +0.7 V, labeled as A_2. In the negative-

going potential scan voltammograms, the peak C_1 appeared resolved into two signals. In contrast, gilded panels produced single peaks A_1, A_2 and C_1, C_2, respectively. These features suggest, in agreement with AFM graphs, that 'young' gold surfaces submitted to more or less intense surface renewal present different electrochemically active sites resulting in peak splitting for the signals A_2/C_2. The overall oxidation of such 'young' surfaces apparently produces two different monolayers of gold oxide(s) resulting in the two-peak reductive response recorded for C_1. It is pertinent to note that, based on studies of single-crystal electrodes, the peak potentials of gold oxidation can be considered as representative of different crystalline planes and defects so that when the single-crystal surfaces have steps and defects, peak multiplicity was observed [42]. Accordingly, abrasive conditioning of gold surfaces will produce multiple surface restructuring/faceting leading to the exposure of domains/planes/defects resulting in the multiple peak voltammetric response.

Our experimental data suggested that the voltammetric features recorded for panel samples presented systematic variations with their age. Figure 8 shows the variation of the ratio between the peak current of the A_2 signal, and the peak current for the process A_1, $i_p(A_2)/i_p(A_1)$, for the samples studied here as a function of the alteration time computed from the date of finishing of the different altarpieces using SWVs such as in Figures 7c,d. One can see that, in spite of relatively large data dispersion, there is a tendency of increasing $i_p(A_2)/i_p(A_1)$ on increasing time. This tendency would be consistent with the idea that, upon prolonging the time of alteration, there is an increase in the number of active Au atoms responsible for the signal A_2. Tentatively, this increase in the active sites can be associated to the environmental attack, in particular, of reactive oxygen species. In recent works, Scholz et al. showed that the attack of $OH^{\bullet}$ radicals generated by the Fenton reaction produced features similar to typical grain boundary corrosion [49-51], whereas annealing of gold at high temperatures (900 ºC) and mechanical treatments (ultrasonication) produced variations of crystallinity, modification in the grain size and formation of gold surfaces with preferred crystallographic orientations [52].

A second feature able to be used for monitoring the aging of the gilded panels can be seen in Figure 9, where SWVs of samples **S2**, **S4**, **S12** and **S16** in contact with 1.0 M

H_2SO_4. One can see in this figure that the peak A_1 for such samples, which correspond to altarpieces dated back in 1482-1484, 1603-1605, 1728 and 1962, respectively, appears to be increasingly smoothed on increasing the age of the sample. Under aging, the peak A_1 becomes smoothed. To quantify this effect, the slope of the modified Tafel representations of $\ln[(i_p-i)/i_p]$ vs. E based on current measurements at different potentials in the central region of the voltammetric peak A_1, was taken. As already described [53], this procedure is less sensitive to the selection of the base line than the conventional Tafel analysis ($\ln(i/i_p)$ vs. E) at the foot of the voltammetric peak.

Data for gilded panels suggest that there is, effectively, a progressive smoothing of gold surfaces under aging. Figure 10 shows the variation with the sample age of the slope of the modified Tafel representations of $\ln[(i_p-i)/i_p]$ vs. E for peak A_1 determined in voltammograms such as in Figure 8. Although there was relatively large data dispersion, a monotonically decreasing tendency was obtained. This feature can be tentatively attributed to the generation of defect sites due to the environmental attack resulting in some restructuring of the gold surface which is reflected in a slight decrease in the rate of the electrochemical generation of the gold oxide monolayer (process A_1). Consistently, the ratio between the peak currents for peaks C_1 and A_1 in CVs (Figure 6) and SWVs (Figure 7), $i_p(C_1)/i_p(A_1)$, was observed to decrease with the age of the samples, as illustrated in Figure 10. This feature can be considered as the result of the superposition of effects associated to the gold oxide formation/reduction and can be considered as consistent with reported experiments cyclic voltammetry on polycrystalline gold electrodes where the height of peak C_1 relative to peak A_1 was enhanced upon repetitive cycling the potential scan resulting in the 'refreshing' and exposition of selected crystal planes of the gold surface [42].

The variation of the above tested parameters with the age of the gilded panels in this study suggests that there is possibility of monitoring the aging process and eventually dating artistic gilded objects using the variation of voltammetric features. This last purpose, however, requires a detailed knowledge of the involved aging processes and the construction of calibration graphs covering an extensive time range [54-57]. Current efforts are devoted to improve the knowledge of the electrochemical signatures of gold aging and study the application to archaeological objects.

Conclusions

The voltammetric response of submicrosamples of gilded panels from altarpieces attached to graphite electrodes in contact with HCl and H_2SO_4 aqueous electrolytes was compared with that of polycrystalline gold electrodes. The samples, providing from churches of the Comunitat Valenciana (Spain), covered a time interval between the 15th century and nowadays. A series of specific features associated to bulk gold and activated gold surfaces were found to vary with the age of the panels thus denoting the possibility of monitoring voltammetrically the aging of the objects and suggesting the possibility of establishing electrochemical criteria for dating.

Ackonwledgements: Financial support from the MINECO Projects CTQ2014-53736-C3-1-P and CTQ2014-53736-C3-2-P which are supported with ERDF funds is gratefully acknowledged. The authors also whish to thank Dr. José Luis Moya López, Mr. Manuel Planes Insausti and Mrs. Alicia Nuez Inbernón (Microscopy Service of the Universitat Politècnica de València) for technical support.

References

[1] Le Goff J (1991) El hombre medieval. Alianza Editorial, Madrid

[2] Valero-Cuenca A (2011) El oro: símbolo de lo trascendente en la pintura gótica. Su capacidad como elemento transformador, espiritual y plástico. Archivo de Arte Valenciano XCII. Real Academia de Bellas Artes de San Carlos, València

[3] Rodriguez-López A, Khandekar N, Gates G, Newman R (2007) Materials and techniques of a Spanish Renaissance panel painting, Stud Conserv 52: 81-100.

[4] Chao R, Heginbotham A, Lee L, Chiari G (2014) Materials and techniques of gilding on a suite of French eighteenth-century chair, Stud Conserv 59: 102-112.

[5] Alfonso-Muñoz M, Ferragut-Adam, X, Guerola-Blay V, Roig-Picazo, MP (2008) Intervención en la ornamentación dorada del espacio central y acceso sur de la Basílica de la Virgen de los Desamparados de Valencia. Arché 3:117–126.

[6] Antonelli F, Lazzarini L, Cancellere S, Tesser E (2016) Study of the deteriortion products, gilding, and polychromy of the stones of the *Scuola Grande Di San Marco*'s façade in Venice, Stud Conserv 61: 74-85.

[7] Toniolo L, Colombo C, Bruni S, Fermo P, Casoli A, Palla G, Bianchi CL (1998) Gilded stuccoes of the Italian baroque, Stud Conserv 43: 201-208.

[8] De Quinto ML (1984) Los batihojas artesanos del oro. Editora Nacional, Madrid

[9] López-Zamora E (2007) Estudio de los materiales y procedimientos del dorado a través de las fuentes literarias antiguas: aplicación en las decoraciones de pinturas castellanas sobre tabla. PhD Thesis. Universidad Complutense de Madrid, Madrid

[10] Herranz E (2000) El arte de dorar, 6th ed, Dossat, Madrid.

[11] Crabbe AC, Giumlia-Mair A, Wouters HJM, Terryn H, Vandendael I (2016) *De Colorando Auro*: Experimenta and literatura study of medieval colouring récipes on gilded plates Stud Conserv 61: 274-285 and references therein.

[12] González E (1997) Tratado del dorado, plateado y su policromía (Tecnología, conservación y restauración). Universitat Politècnica de València, València.

[13] Baixauli-Juan I (2001) Els artesans de la València del segle XVII: Capítols dels oficis i col·legis, Universitat de València, València

[14] Mocholí-Roselló A (2012) Pintors i artífex de la València medieval. Universitat Politècnica de València, València

[15] Doménech-Carbó A, Doménech-Carbó MT, Costa V (2009) Electrochemical Methods in Archaeometry, Conservation and Restoration. Monographs in Electrochemistry Series, Scholz F, Ed. Springer, Berlin-Heidelberg.

[16] Melo HP, Cruz AJ, Candelas A, Mirao J, Cardoso AM, Oliveira MJ, Valadas S (2014) Problems of Analysis by FTIR of Calcium Sulphate–Based Preparatory Layers: The Case of a Group of 16th-Century Portuguese Paintings, Archaeometry 56:513–526

[17] Picollo M, Fukunaga K, Labaune J (2015) Obtaining noninvasive stratigraphic details of panel paintings using terahertz time domain spectroscopy imaging system. J Cult Herit 16: 73–80

[18] Duran A, Perez-Rodríguez JL, Jimenez de Haro MC, Herrera LK, Justo A (2008) Degradation of gold and false golds used as gildings in the cultural heritage of Andalusia, Spain, J Cult Herit 9:184-188

[19] Gulotta D, Goidanich S, Bertoldi M, Bortolotto S, Toniolo L (2012) Gildings and false gildings of the baroque age: characterization and conservation problems. Archaeometry 54:940–954

[20] Constantinescu B, Vasilescu A, Radtke M, Reinholz U (2010) Micro-SR-XRF studies for archaeological gold identification—the case of Carpathian gold and Romanian museal objects. Appl Phys A 99:383–389

[21] Scholz F, Meyer B (1998) Voltammetry of solid microparticles immobilized on electrode surfaces, Electroanalytical Chemistry, A Series of Advances. Bard AJ, Rubinstein I, Eds., Marcel Dekker, New York, vol. 20, pp 1–86

[22] Scholz F, Schröder U, Gulaboski R, Doménech-Carbó A (2014) Electrochemistry of Immobilized Particles and Droplets, 2nd Edit. Springer, Berlin-Heidelberg.

[23] Doménech-Carbó A, Labuda J, Scholz F (2013) Electroanalytical chemistry for the analysis of solids: characterization and classification (IUPAC Technical Report), Pure Appl Chem 85:609–631.

[24] Doménech-Carbó A (2010) Voltammetric methods applied to identification, speciation and quantification of analytes from works of art: an overview. J Solid State Electrochem 14:363–369

[25] Doménech-Carbó A (2011) Tracing, authentifying and dating archaeological metal using the voltammetry of microparticles. Anal Methods 3:2181–2188

[26] Doménech-Carbó A, Doménech-Carbó MT, Peiró-Ronda MA, Osete-Cortina L (2011) Authentication of archaeological lead artifacts using voltammetry of microparticles: the case of the *Tossal de Sant Miquel* Iberian plate. Archaeometry 53:1193–1211

[27] Doménech-Carbó A, Doménech-Carbó MT, Martínez-Lázaro I (2008) Electrochemical identification of bronze corrosion products in archaeological artefacts. A case study. Microchim Acta 162:351–359

[28] Satovic D, Martinez S, Bobrowski A (2010) Electrochemical identification of corrosion products on historical and archaeological bronzes using the voltammetry of micro-particles attached to a carbon paste electrode. Talanta 81:1760–1765

[29] Doménech-Carbó A, Doménech-Carbó MT, Martínez-Lázaro I (2010) Layer-by-layer identification of copper alteration products in metallic works of art using the voltammetry of microparticles approach. Anal Chim Acta 610:1–9

[30] Cepriá G, Abadías O, Pérez-Arantegui J, Castillo JR (2001) Electrochemical behavior of silver-copper alloys in voltammetry of microparticles: a simple method for screening purposes. Electroanalysis 13:477–483

[31] Doménech-Carbó A, Doménech-Carbó MT, Pasíes T, Bouzas MC (2012) Modeling corrosion of archaeological silver-copper coins using the voltammetry of immobilized particles. Electroanalysis 24:1945–1955

[32] Capelo S, Homem PM, Cavalheiro J, Fonseca ITE (2013) Linear sweep voltammetry: a cheap and powerful technique for the identification of the silver tarnish layer constituent. J Solid State Electrochem 17:223–234

[33] Doménech-Carbó A, Del Hoyo-Rodríguez J, Doménech-Carbó MT, Piquero-Cilla J (2017) Electrochemical analysis of the first Polish coins using the voltammetry of immobilized particles. Microchem J 130:47–55

[34] Ferragud X (2015) Estudi de les tècniques del daurat i la policromia sobre l'or a l'escola valenciana del segle XV al segle XIX Analisi dels materials, tècniques i procediments. PhD Thesis, University of Valencia.

[35] Burke LD, Nugent PF (1997) The electrochemistry of gold: I the redox behaviour of the metal in aqueous media. Gold Bull 30:43–53

[36] Chen A, Lipkowski J (1999) Electrochemical and Spectroscopic Studies of Hydroxide Adsorption at the Au(111) Electrode. J Phys Chem B 103:682–691

[37] Hoogvliet JC, van Bennekom WP (2001) Gold thin-film electrodes: an EQCM study of the influence of chromium and titanium adhesion layers on the response. Electrochim. Acta 47:599–611

[38] Burke LD, O'Mullane AP (2000) Generation of active surface states of gold and the role of such states in electrocatalysis. J Solid State Electrochem 4:285–297

[39] Burke LD, O'Mullane AP, Lodge VE, Mooney MB (2001) Auto-inhibition of hydrogen gas evolution on gold in aqueous acid solution. J Solid State Electrochem 5: 319–327

[40] Doménech-Carbó A, Doménech-Carbó MT, Osete-Cortina L (2004) Electrochemistry of archaeological metals: an approach from the voltammetry of microparticles, en "Trends in electrochemistry and corrosion at the beginning of the 21st century (dedicated to Professor Dr. Josep M. Costa on the occasion of his 70th birthday); Brillas E, Cabot P-L, Eds. Universitat de Barcelona, Barcelona, pp. 857–871

[41] Doyle RL, Lyons MEG (2014) The mechanism of oxygen evolution at superactivated gold electrodes in aqueous alkaline solution. J Solid State Electrochem 18:3271–3286

[42] Jeyabharathi C, Hasse U, Ahrens P, Scholz F (2014) Oxygen electroreduction on polycrystalline gold electrodes and on gold nanoparticle-modified glassy carbon electrodes. J Solid State Electrochem 18:3299–3306.

[43] Jeyabharathi C, Ahrens P, Hasse U, Scholz F (2016) Identification of low-index crystal planes of polycrystalline gold on the basis of electrochemical oxide layer formation. J. Solid State Electrochem 20:3025–3031

[44] Cherevko S, Kulyk N, Chung C-H (2012) Utilization of surface active sites on gold in preparation of highly reactive interfaces for alcohols electrooxidation in alkaline media. Electrochim Acta 69:190–196

[45] Doménech-Carbó A, Doménech-Carbó MT, Peiró-Ronda MA (2011) 'One-touch' voltammetry of microparticles for the identification of corrosion products in archaeological lead. Electroanalysis 23:1391–1400

[46] Blum D, Leyffer W, Holze R (1996) Pencil-Leads as New Electrodes for Abrasive Stripping Voltammetry. Electroanalysis 8:296–297

[47] Izumi T, Watanabe I, Yokoyama Y (1991) Activation of a gold electrode by electrochemical oxidation-reduction pretreatment in hydrochloric acid. J Electroanal Chem Interfacial Electrochem 303:151–160

[48] Mesgar M, Kaghazchi P, Jacob T, Pichardo-Pedrero E, Giesen M, Ibach H, Luque NB, Schmickler W (2013) Chlorine-enhanced surface mobility of Au(100). ChemPhysChem 14:233–236

[49] Scholz F, López de Lara González G, de Carvalho LM, Hilgemann M, Brainina Kh Z, Kahlert H, Jack RS, Minh DT (2007) Indirect Electrochemical Sensing of Radicals and Radical Scavengers in Biological Matrices. Angew Chem Int Ed 46:8079–8081

[50] Nowicka A, Hasse U, Sievers G, Donten M, Stojek Z, Fletcher S, Scholz F (2010) Selective Knockout of Gold Active Sites. Angew Chem Int Ed 49:3006–3009

[51] Hasse U, Fricke K, Dias D, Sievers G, Wulff H, Scholz F (2012) Grain boundary corrosion of the surface of annealed thin layers of gold by OH·radicals. J Solid State Electrochem 16:2383–2389

[52] Hasse U, Wulff H, Helm CA, Scholz F (2013) Formation of gold surfaces with a strongly preferred {100}-orientation. J Solid State Electrochem 17:3047–3053

[53] Doménech-Carbó A, Doménech-Carbó MT, Pasíes T, Bouzas MC (2011) Application of modified Tafel analysis to the identification of corrosion products on archaeological metals using voltammetry of microparticles. Electroanalysis 23:2803–2812.

[54] Doménech-Carbó A, Doménech-Carbó MT, Peiró-Ronda MA (2011) Dating archaeological lead artifacts from measurement of the corrosion content using the voltammetry of microparticles. Anal Chem 83:5639–5644

[55] Doménech-Carbó A, Doménech-Carbó MT, Peiró-Ronda MA, Martinez-Lázaro I, Barrio J (2012) Application of the voltammetry of microparticles for dating archaeological lead using polarization curves and electrochemical impedance spectroscopy. J Solid State Electrochem 16:2349–2356

[56] Doménech-Carbó A, Doménech-Carbó MT, Capelo S, Pasíes T, Martínez-Lázaro I (2014) Dating archaeological copper/bronze artifacts using the voltammetry of microparticles. Angew Chem Int Ed 53:9262–9266

[57] Doménech-Carbó A, Capelo S, Piquero J, Doménech-Carbó MT, Barrio J, Fuentes A, Al-Sekkaneh W (2016) Dating archaeological copper using electrochemical impedance spectroscopy. Comparison with voltammetry of microparticles dating. Mater Corr 67:120–129

Table 1. Location and age of gilded panel samples in this study.

Sample	Description/Location of Altarpieces	Author	Date
S1	*Retaule de la Verge de l'Esperança*, *Santa Maria* church, Pego	Antoni Peris	1400-1405
S2	*Retaule de la Verge de Gràcia*, *Sant Miquel Arcángel* church, Enguera	Paolo de San Leocadio	1482-1484
S3	*Retaule de la Verge de Gràcia*, *Nostra Senyora de Gràcia* church, Rugat	Nicolau Borràs	ca. 1600
S4	*Taules de Sant Vicent*, *Sant Jaume church*, Algemesí	Francisco Ribalta	1603-1605
S5	Organ, *Sant Jaume* church, Algemesí	Gabriel Ximénez	ca. 1609
S6	*Retaule de Sant Martí*, *Sant Martí* church, Sogorb	Francisco Pérez	1630
S7	*Retaule de les Ànimes*, *Sant Martí* church, Sogorb	Workshop of Francisco Pérez	ca. 1625
S8	*Retaule de Santa Úrsula*, *Sant Martí* church, Sogorb	Workshop of Francisco Pérez	ca. 1625
S9	*Retaule del Calvari*, Lluis Vives Institute, Valencia	Anonymous	ca. 1675
S10	*Retaule de Sant Pau*, Lluis Vives Institute, Valencia	Tomás Artigues	1723
S11	*Retaule de la Pietat*, Lluis Vives Institute, Valencia	Anonymous	1723
S12	*Retaule de Sant Josep*, *L'Assumpció* church, Torrent	Andreu Robres	1728
S13	*Floró de la Capella de la Comunió*, *Sant Roc* church, Oliva	Anonymous	1749
S14	*Retaule de la Verge de la Misericordia*, *Nostra Senyora de la Misericordia* church, Banyeres	Ramón Porta	1947
S15	*Retaule de Sant Vicent*, *Sant Jaume* church, Algemesí	Ramón Porta	1954
S16	*Retaule de Sant Bernat*, *Santa Caterina* church, Alzira	Elías Cuñat	1962

Figures

Figure 1. Altarpiece of Saint Joseph in the *L'Assumpció* church, Torrent (Valencia, Spain) performed by Andreu Robres, 1728.

Figure 2. Microphotographs of sample **S9**: a) Optical microscopy image of a cross section (reflected episcopic illumination); b) secondary electron image of the same cross section obtained with FESEM; c) EDX spectrum of the gold leaf. 1: Gold leaf; 2: preparative layer of bole; 3: outer ground prepared with fine gesso; 4: inner ground prepared with gross gesso.

Figure 3. Representation of the values of the percentage (wt) of MgO in the bole layer (squares) and the percentage of Ag (wt) in the gold leaf (triangles) vs. the values of the percentage (wt) of Al_2O_3 in the bole layer of the studied samples. Inset: geographical distribution of the altarpieces in the territory of the *Comunitat Valenciana* (Spain).

Figure 4. Amplitude error AFM topological maps for: a) contemporary gold leaf and b) sample of gilding from the *Verge de la Misericordia* Altarpiece, *Nostra Senyora de la Misericordia* church, Banyeres (1947).

Figure 5. CVs of a,b) pristine polycrystalline gold electrodes, c) polycrystalline gold electrode after glossy with an agate burnisher, and d) gold leaf sample attached to graphite electrode, in contact with air-saturated a,b) 0.10 M H_2SO_4 and c,d) 0.10 M HCl aqueous solution. Potential initiated at 0.0 V in the positive direction; potential scan rate of 50 mV s^{-1}.

Figure 6. CVs, after semi-derivative deconvolution of graphite electrodes: a) unmodified; b) modified with gold leaf; c) modified with sample **S6** in contact with 0.10 M HCl. CVs: Potential initiated at 0.0 V in the positive direction and scanned between +1.25 and –0.65 V at a scan rate of 50 mV s^{-1}. Notice that only the region between 0.0 and +1.25 V of CVs was depicted.

Figure 7. SWVs of a) polycrystalline gold electrode abrasively conditioned and graphite electrodes modified with b) burnished gold leaf (mechanical conditioning with

agate burnisher), c) sample **S10** (1723) and d) sample **S1** (1405) in contact with air-saturated 1.0 M H_2SO_4. Potential scan initiated at +1.45 V in the negative direction (black lines) and -0.05 V in the positive direction (red lines); potential step increment 4 mV; square wave amplitude 25 mV; frequency 5 Hz. Dotted lines represent the base lines used for peak current measurement.

Figure 8. Variation of the peak current ratio $i_p(A_2)/i_p(A_1)$ with the age of the gilded panel samples in this study. From SWV data in 1.0 M H_2SO_4 in conditions such as in Figure 6c,d.

Figure 9. SWVs of samples a) **S2**, b) **S4**, c) **S12** and d) **S16** attached to graphite bars in contact with 1.0 M H_2SO_4. Potential scan initiated at –0.05 V in the positive direction; potential step increment 4 mV; square wave amplitude 25 mV; frequency 5 Hz. Dotted lines represent the base lines for current measurements.

Figure 10. Variation with the sample age of the slope of the modified Tafel representations of $\ln[(i_p-i)/i_p]$ vs. E for peak A_1 determined in voltammograms such as in Figure 9.

Figure 11. Variation with the age of the ratio between the peak current ratio $i_p(C_1)/i_p(A_1)$ in SWVs such as in Figure 7 of sample-modified graphite electrodes in contact with 1.0 M H_2SO_4.

Figure 1.

Figure 2.

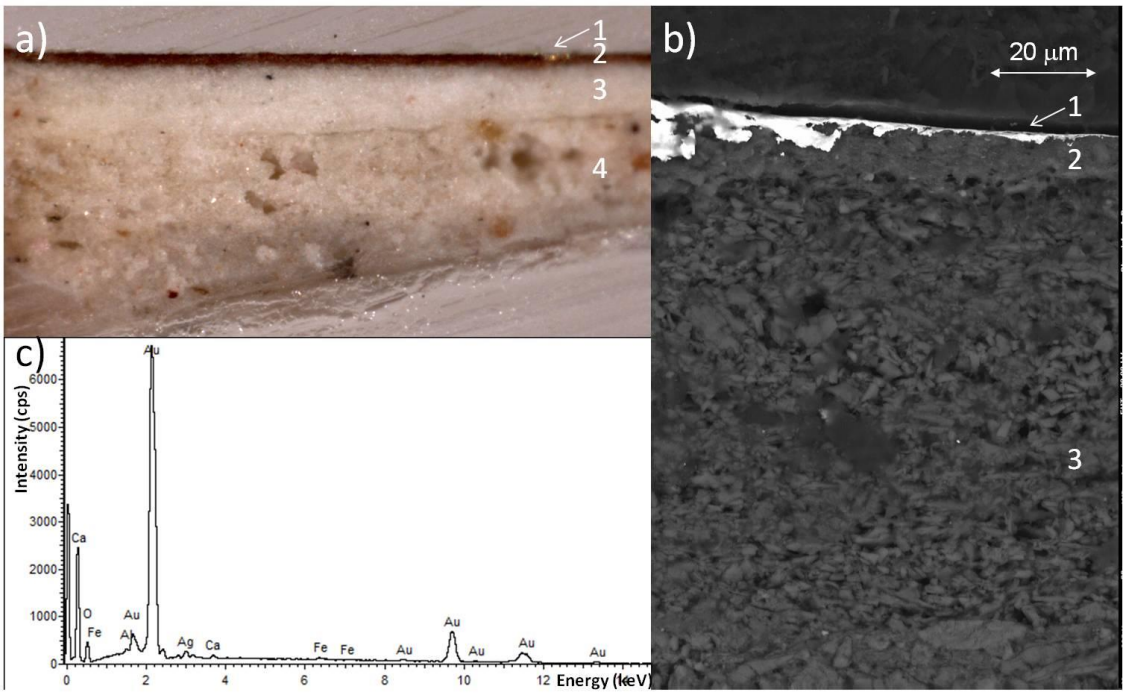
a)
1
2
3
4
b)
20 μm
1
2
3
c)
Intensity (cps)
Energy (keV)
Ca
O
Fe
Au
Ag
Ca
Fe
Fe
Au
Au
Au
Au

Figure 3.

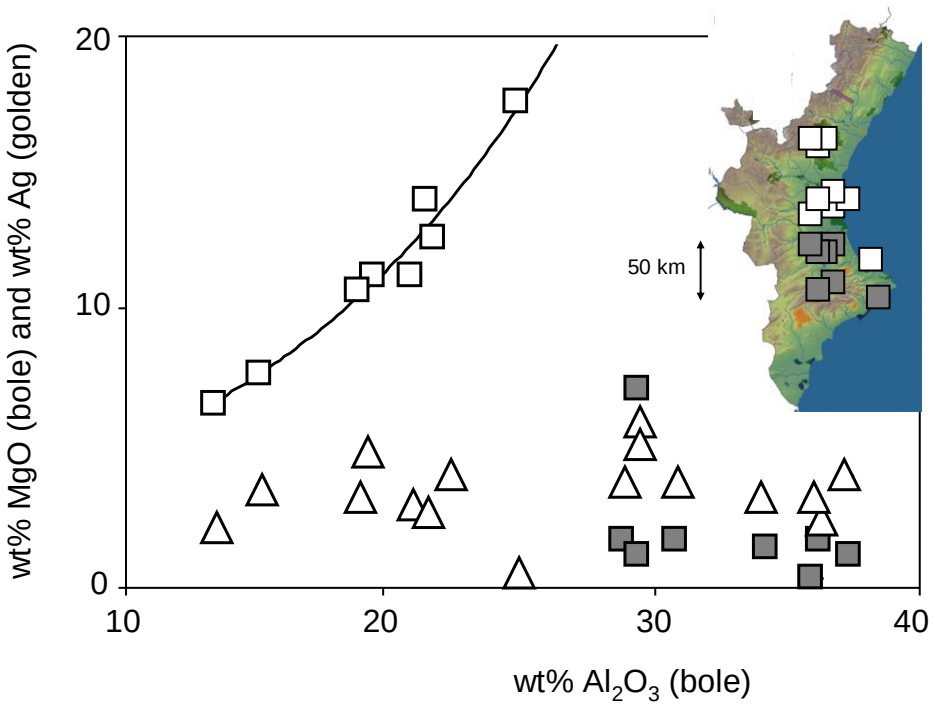
20
10
0
10
20
30
40
wt% MgO (bole) and wt% Ag (golden)
wt% Al_2O_3 (bole)
50 km

Figure 4.

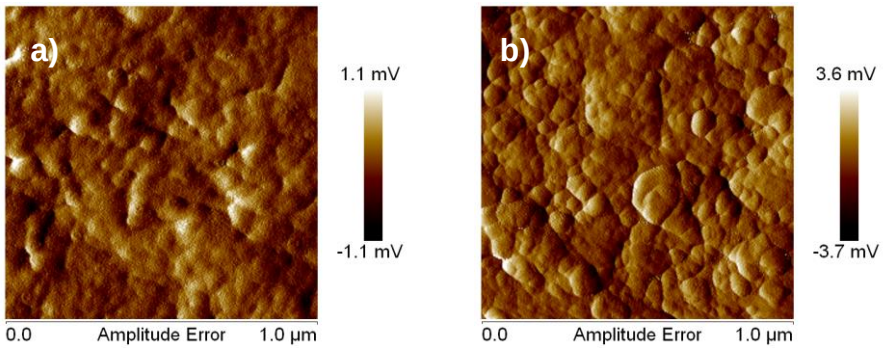
a)
1.1 mV
-1.1 mV
0.0
Amplitude Error
1.0 µm
b)
3.6 mV
-3.7 mV
0.0
Amplitude Error
1.0 µm

Figure 5.

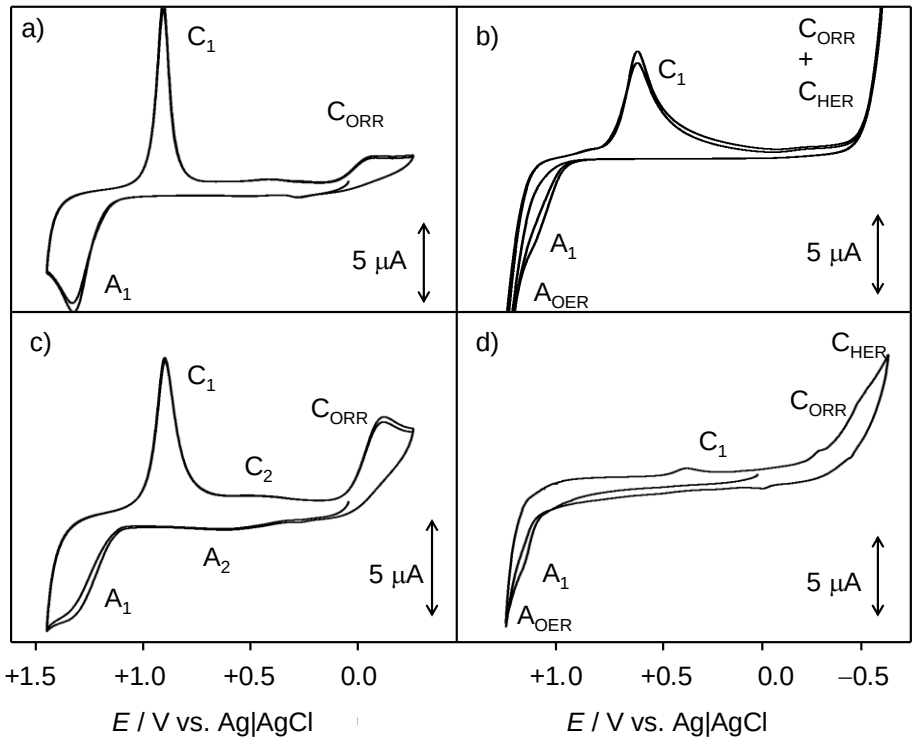
a)
C1
CORR
A1
5 μA
b)
CORR
+
CHER
C1
A1
AOER
5 μA
c)
C1
CORR
C2
A2
A1
5 μA
d)
CHER
CORR
C1
A1
AOER
5 μA
+1.5
+1.0
+0.5
0.0
E / V vs. Ag|AgCl
+1.0
+0.5
0.0
–0.5
E / V vs. Ag|AgCl

Figure 6.

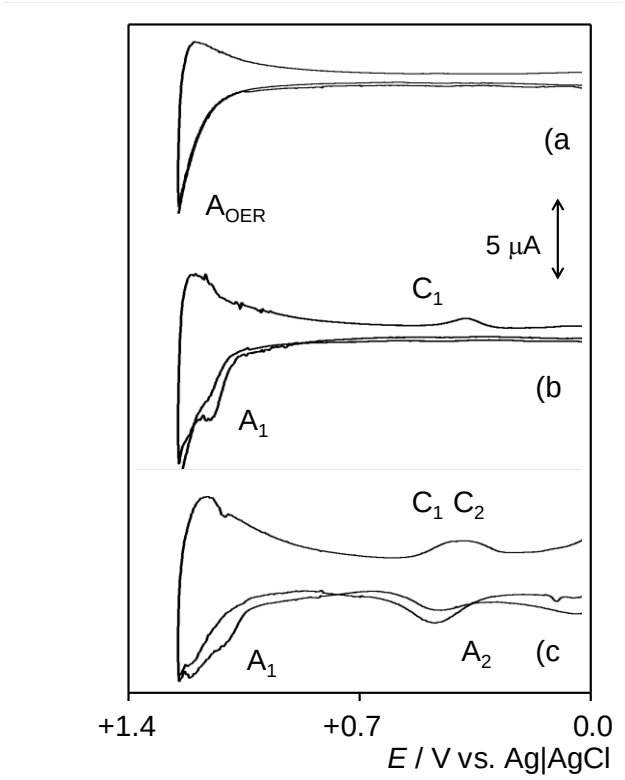

Figure 7.

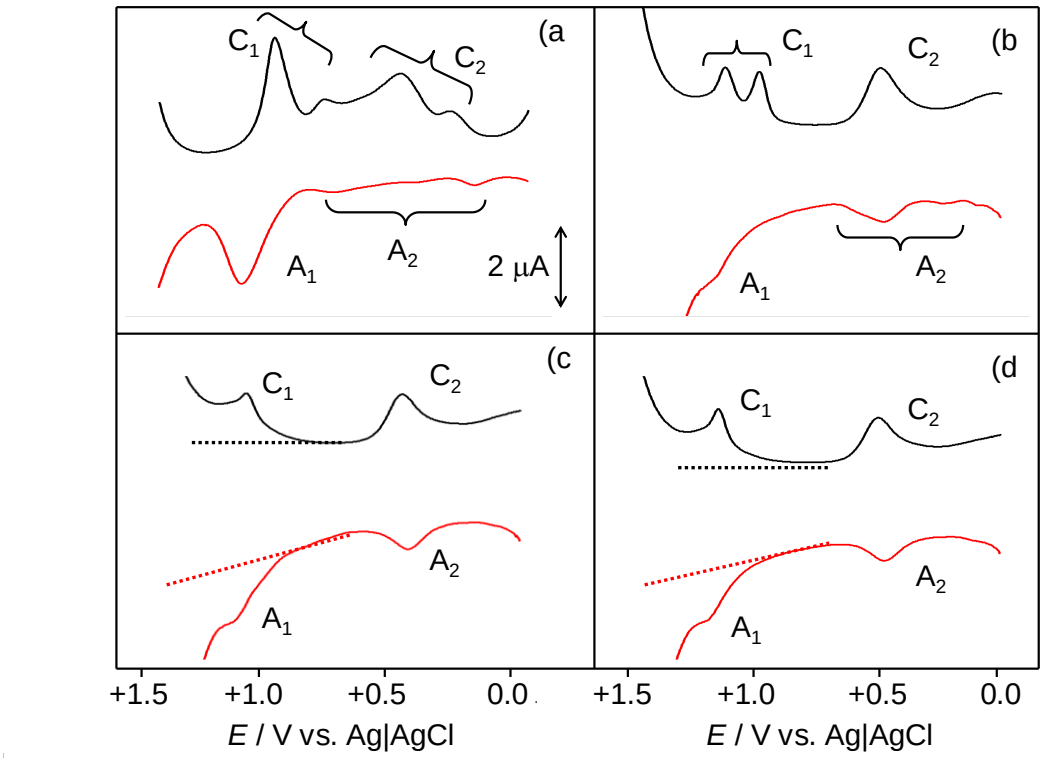
(a
C1
C2
A1
A2
2 μA
(b
C1
C2
A1
A2
(c
C1
C2
A1
A2
(d
C1
C2
A1
A2
+1.5
+1.0
+0.5
0.0
E / V vs. Ag|AgCl
+1.5
+1.0
+0.5
0.0
E / V vs. Ag|AgCl

Figure 8.

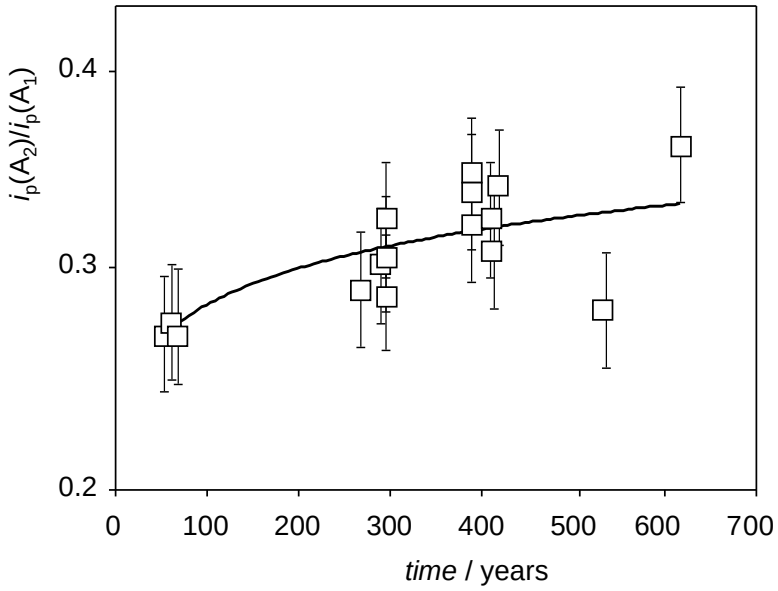

Figure 9.

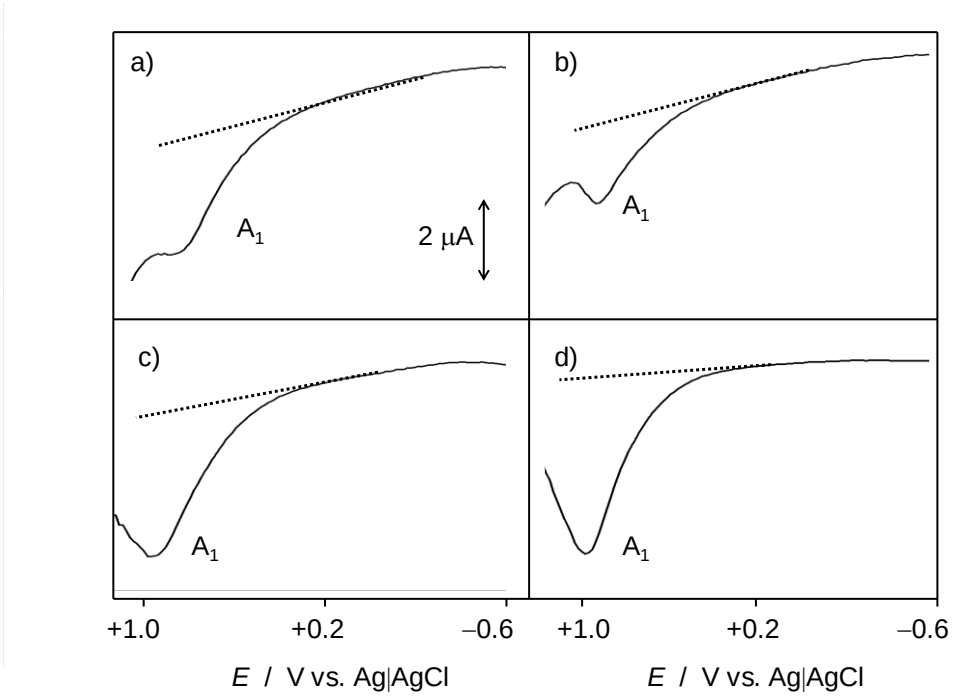

Figure 10.

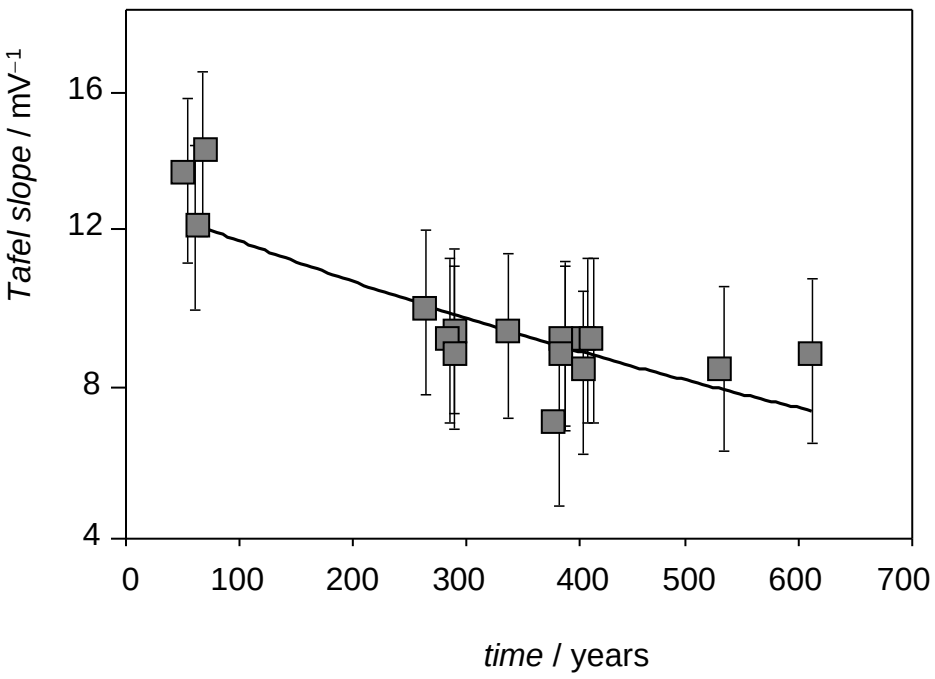
Tafel slope / mV⁻¹
16
12
8
4
0
100
200
300
400
500
600
700
time / years

Figure 11.

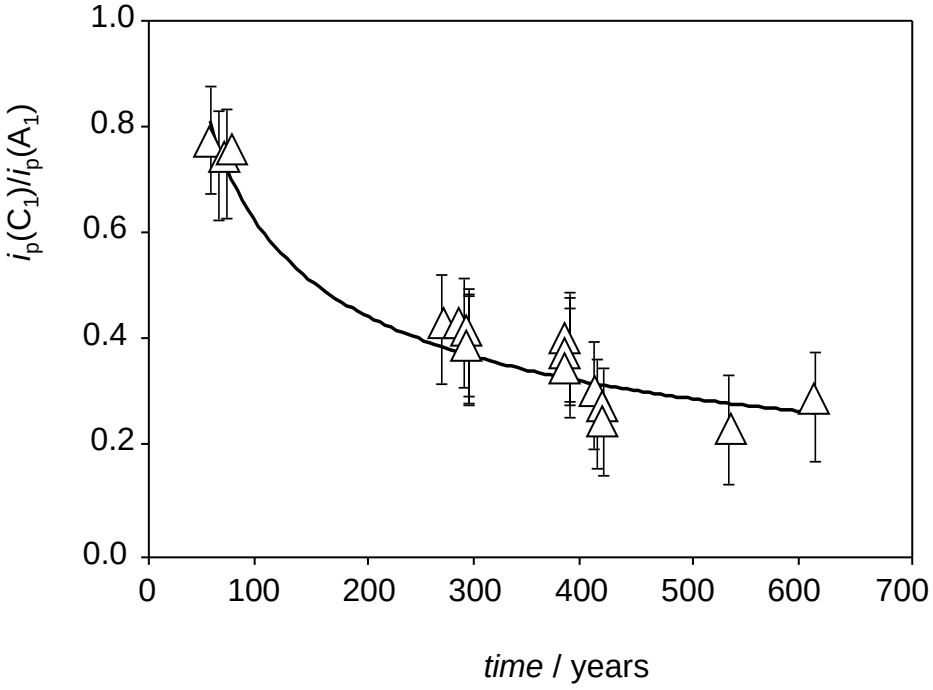
1.0
0.8
0.6
0.4
0.2
0.0
$i_p(C_1)/i_p(A_1)$
0
100
200
300
400
500
600
700
time / years